results in the GSM-900, the GSM-1800/1900, and the 802.11b/g interferers can be rejected effectively. Moreover, excellent input impedance matching over the band of interest can also be achieved due to the intrinsic wideband matching characteristics of the proposed passive BP-filter. The excellent measurement results indicate that the proposed LNA architecture is suitable for low-power 3–10-GHz UWB communication systems.

ACKNOWLEDGMENTS

This work is supported by the National Science Council of the R.O.C. under Contracts NSC 97-2221-E-260-009-MY3 and NSC 97-2221-E-260-010-MY3. The authors are very grateful for the support from National Chip Implementation Center (CIC), Taiwan, for chip fabrication, and Dr. Guo- Wei Huang, National Nano-Device Laboratory (NDL), Taiwan, for high-frequency measurements.

REFERENCES

1. S. Lo, I. Sever, S.P. Ma, P. Jang, A. Zou, C. Arnott, K. Ghatak, A. Schwartz, L. Huynh, V.T. Phan, and T. Nguyen, A dual-antenna phased-array UWB transceiver in 0.18-μm CMOS, IEEE J Solid--State Circuits 41 (2006), 2776–2786.
2. T.W. Fischer, B. Kelleci, K. Shi, A.I. Karsilayan, and E. Serpedin, An analog approach to suppressing in-band narrow-band interference in UWB Receivers, IEEE Trans Circ Syst I Reg Papers 54 (2007), 941–950.
3. C.P. Liang, P.Z. Rao, T.J. Huang, and S.J. Chung, Analysis and design of two low-power ultra-wideband CMOS low-noise amplifiers with out-band rejection, IEEE Trans Microwave Theory Tech 58 (2010), 277–286.
4. Y. Gao, Y.J. Zheng, and B.L. Ooi, 0.18 μm CMOS dual-band UWB LNA with interference rejection, IET Electron Lett 43 (2007), 1096–1098.
5. A. Bevilacqua, A. Vallese, C. Sandner, M. Tiebout, A. Gerosa, and A. Neviani, A 0.13 μm CMOS LNA with integrated balun and notch filter for 3 to 5 GHz UWB receivers, IEEE International Solid-State Circuits Conference, San Francisco, CA, pp. 420–421, 2007.
6. S.K. Tang, K.P. Pun, C.S. Choy, C.F. Chan, and K.N. Leung, A fully differential band-selective low-noise amplifier for MB-OFDM UWB receivers, IEEE Trans Circ Syst II: Exp Briefs 55 (2008), 653–657.
7. M.C. Lu, J.F. Chang, Y.S. Lin, and L.C. Lu, 1.89 dB insertion-loss UWB BP-filter with three finite transmission zeros using standard 0.18 μm CMOS technology, IET Electron Lett 45 (2009), 56–57.
8. M.J. Wu, J.N. Yang, and C.Y. Lee, A constant power consumption CMOS LC oscillator using improved high-Q active inductor with wide tuning-range, Proc. IEEE 47th Midwest Circuits Syst. Symp., July 2004, Vol. 3, pp. 347–350.
9. M.L. Edwards and J.H. Sinsky, A new criterion for linear 2-port stability using a single geometrically derived parameter, IEEE Trans Microwave Theory Tech 40 (1992), 2303–2311.
10. D. Barras, F. Ellinger, H. Jackel, and W. Hirt, A low supply voltage SiGe LNA for ultra-wideband frontends, IEEE Microwave Wireless Compon Lett 14 (2004), 469–471.
11. J.Y. Lin and H.K. Chiou, Power-constrained third-order active notch filter applied in IR-LNA for UWB standards, IEEE Trans Circ Syst II: Exp Briefs 58 (2011), 11–15.
12. B. Park, S. Choi, and S. Hong, A low-noise amplifier with tunable interference rejection for 3.1- to 10.6-GHz UWB systems, IEEE Microwave Wireless Compon Lett 20 (2010), 40–42.
13. C.F. Liao and S.I. Liu, A broadband noise-canceling CMOS LNA for 3.1–10.6-GHz UWB receivers, IEEE J Solid-State Circ 42 (2007), 329–339.
14. K.H. Chen, J.H. Lu, B.J. Chen, and S.I. Liu, An ultra-wide-band 0.4–10-GHz LNA in 0.18-μm CMOS, IEEE Trans Circ Syst II: Exp Briefs 54 (2007), 217–221.

HYBRID INTEGRATION OF 4-W AND 8-W S-BAND GaN POWER AMPLIFIERS ON A SELECTIVELY ANODIZED ALUMINUM SUBSTRATE

Dong-Wook Kim
Department of Radio Science and Engineering, Chungnam National University, 220 Gung-Dong, Yuseong-Gu, Daejeon 305-764, Republic of Korea; Corresponding author: dwkim21c@cnu.ac.kr

Received 13 July 2011

ABSTRACT: *Hybrid integration of 4-W and 8-W GaN power amplifiers operating in 2–3 GHz is attempted on a selectively anodized aluminum substrate. Discrete GaN high electron mobility transistors are inserted in selectively etched pockets of the aluminum metal substrate and all passive matching circuits are fabricated on the anodized aluminum oxide layer of the aluminum substrate. The 4-W power amplifier shows a flat gain of 20–23 dB in 0.7–4.5 GHz, a maximum output power of 37.5 dBm at 2.5 GHz, and output power variation of ±0.35 dB in 2–3 GHz. The 8-W power amplifier also shows a maximum output power of 39.6 dBm at 2.5 GHz and output power variation of ±0.5 dB in 2–3 GHz.*
 Microwave Opt Technol Lett 54:1261–1263, 2012; View this article online at wileyonlinelibrary.com. DOI 10.1002/mop.26750

Key words: *hybrid integration; GaN high electron mobility transistor; power amplifier; anodized aluminum; etched pocket*

1. INTRODUCTION

A wide bandgap GaN high electron mobility transistor (HEMT) is a very promising device for high-frequency power amplification due to its excellent material and device properties such as high breakdown voltage, high output power density, and high input/output impedance. Its potential has been demonstrated in various ways by many researchers in the last decade [1–4]. Although GaN devices are being actively studied, low-cost and high-quality RF substrates such as an oxidized Si wafer or organic substrate have received much interest from many researchers who wanted to implement large-size passive devices on a low-cost alternative substrate instead of an expensive gallium arsenide (GaAs) or lossy Si wafer [5–7]. Recently, a new RF substrate manufacturing technology that makes a thick anodized aluminum oxide layer (Al_2O_3) on a very cheap aluminum metal plate was introduced for microwave power module packaging [8]. Hybrid integration of GaN HEMTs for high-power amplification and the selectively anodized aluminum substrate for efficient heat sinking is well suited to repeaters or base stations for wireless communications such as Worldwide Interoperability for Microwave Access and Wireless Local Area Network requiring stringent cost reduction.

In this work, with the hybrid integration of GaN HEMTs and the anodized aluminum substrate, 4-W and 8-W power amplifiers operating in 2–3 GHz are introduced. The anodized aluminum oxide layer is 80-μm thick and its relative dielectric constant is 6.7, where all the matching circuits are fabricated using a Cu/benzocyclobutene integrated passive process.

2. CIRCUIT DESIGN

A 4-W and 8-W two-stage power amplifiers are designed using TriQuint GaN HEMTs (TGF2023-01 for 4 W and TGF2023-02 for 8 W) and their schematic circuit is shown in Figure 1(a). To secure stability of the circuit, NiCr gate bias resistors of 150 Ω are shunt-connected because GaN transistors are susceptible to

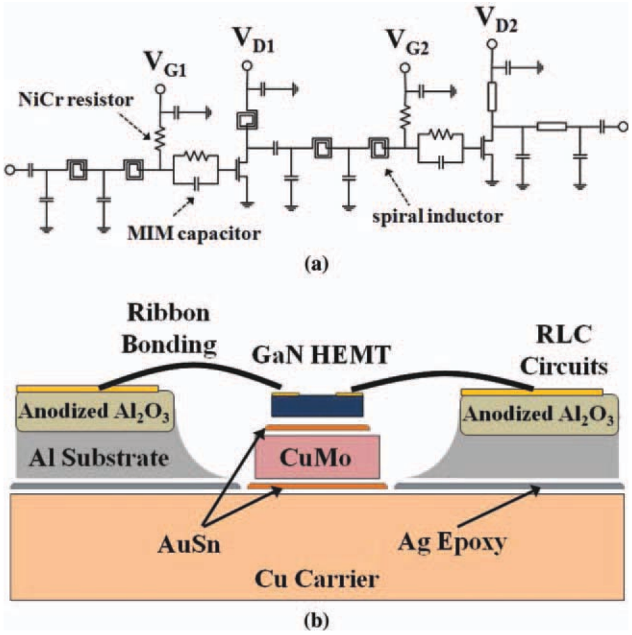

Figure 1 A schematic circuit of the two-stage GaN power amplifier and conceptual illustration of GaN HEMT packaging in the etched pocket of the anodized aluminum substrate. (a) A schematic circuit and (b) GaN HEMT packaging. [Color figure can be viewed in the online issue, which is available at wileyonlinelibrary.com]

unwanted oscillation. Parallel circuits of a NiCr resistor and metal–insulator–metal (MIM) capacitor are series connected to the transistor gates to obtain a flat gain in a wide frequency range by damping high gain at low frequencies. Cascaded L-type circuits of spiral inductors and MIM capacitors are used for interstage matching, and an output matching circuit is optimized for output power. The *S*-parameter simulations and loadpull simulations are performed on Agilent Advanced Design System using a GaN EEHEMT model, which is provided by TriQuint Semiconductor. According to the loadpull simulation, inductive impedance loading at the second harmonic frequency slightly degrades the output power of the amplifier, so output load impedance is designed to provide not only optimal power condition at the fundamental frequency but also capacitive impedance at the lowest second harmonic frequency, 4 GHz, and low resistive impedance at the highest second harmonic frequency, 6 GHz.

The passive matching circuits are integrated on a selectively anodized aluminum oxide layer of the low-cost electro-polished aluminum metal substrate, but discrete GaN HEMTs are inserted in etched pockets of the aluminum substrate and mounted on CuMo carriers as shown in Figure 1(b). The pockets are formed by chemically etching the thinned aluminum substrate after doing the backside lapping of the substrate up to 200 μm [9].

3. MEASUREMENT RESULTS

Figure 2 shows a microphotograph of the fabricated 4-W and 8-W GaN power amplifiers. As shown in the figure, GaN HEMTs are directly attached on CuMo carriers inside the pockets. The labels in Figure 2 indicate the anodized aluminum oxide layer, etched pocket, and GaN HEMTs. The sizes of the fabricated hybrid integrated circuits are 9.3×3 mm^2 for the 4-W amplifier (upper in the figure) and 9.3×3.8 mm^2 for the 8-W amplifier (lower in the figure).

Figure 3(a) shows *S*-parameter measurement results of the 4-W power amplifier, each transistors of which are biased at $V_{DS} = 30$ V and $I_{DS} = 100$ mA. The amplifier has a flat gain of 20–23 dB in 0.75–4.5 GHz and input voltage standing wave ratio (VSWR) less than 2 in 2–3 GHz. Compared with the expected value in the simulation, the gain is decreased by about 5 dB, in part due to a thermal problem caused from DC bias voltage and current. Thanks to resistance-capacitance (RC) parallel circuits at the gates of GaN HEMTs, the amplifier shows wideband gain performance for small-signal operation. Figure 3(b) shows *S*-parameter measurement results of the 8-W power amplifier. The GaN transistor of the first stage is biased at $V_{DS} = 27$ V and $I_{DS} = 100$ mA, and the transistor of the second stage at $V_{DS} = 30$ V and $I_{DS} = 230$ mA. The amplifier shows a slowly decreasing gain of 27–21 dB and input VSWR less than 2 in 2–3 GHz. Overall, the gain is slightly decreased compared with the simulation, where VSWRs show similar performance.

Figure 4 shows output power performance of both power amplifiers with input power at 2.5 GHz and also their saturated output power variation in 2–3 GHz, where graphs are grouped by A (left axis) and B (right axis). In the group A graphs, the 4-W GaN power amplifier has a maximum output power of 37.5 dBm and a power gain of 18.5 dB (not a linear gain) at 2.5 GHz when its first-stage transistor is biased at V_{DS} =27 V and $I_{DS} = 110$ mA and the second-stage transistor at V_{DS} =30 V and $I_{DS} = 120$ mA. A maximum output power of 39.6 dBm and a power gain of 19.6 dB are also obtained in the measurement of the 8-W power amplifier when the first-stage GaN transistor is biased at V_{DS} =27 V and $I_{DS} = 100$ mA and the second-stage transistor at V_{DS} =30 V and $I_{DS} = 210$ mA. The group B graphs show frequency dependence of the saturated output power of both amplifiers. The 4-W amplifier shows the output power variation of 36.4–37.1 dBm in 2–3 GHz with the input power of 18 dBm, whereas the 8-W power amplifier has the output power variation of 38.5–39.6 dBm in the same frequency region. Both amplifiers have relatively uniform saturated output power within 0.5 dB deviation at 2 dB or more compression points in 2–3 GHz.

4. CONCLUSIONS

The hybrid integration of the discrete GaN HEMTs and low-cost anodized aluminum substrates with the etched pockets was

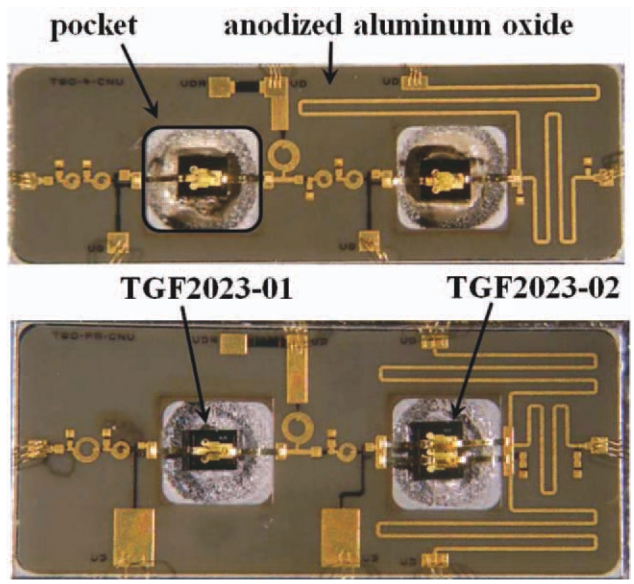

Figure 2 Microphotographs of the 4-W and 8-W power amplifiers fabricated on the anodized aluminum substrate. The upper chip is the 4-W amplifier and the lower chip is the 8-W amplifier. [Color figure can be viewed in the online issue, which is available at wileyonlinelibrary.com]

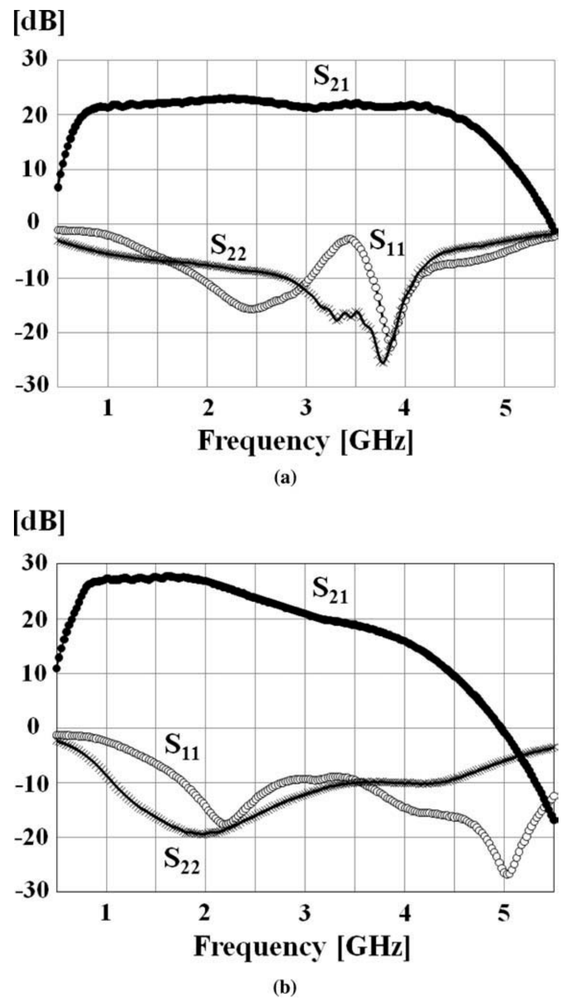

Figure 3 *S*-parameter measurement results of the fabricated GaN power amplifiers. (a) A 4-W power amplifier and (b)a 8-W power amplifier

attempted for the 4-W and 8-W S-band GaN power amplifiers and was successfully demonstrated. The *S*-parameter measurement of both GaN power amplifiers showed wideband gain performance and 2:1 input VSWR in 2–3 GHz. In the power measurement at 2.5 GHz, the 4-W and 8-W power amplifiers showed the maximum output power of 37.5 and 39.6 dBm, respectively, and the saturated output power variation less than 0.5 dB in 2–3 GHz, which meant they had the fractional bandwidth of 40%. The developed GaN power amplifiers could be effectively used in the repeaters and base stations for wireless communications in 2–3 GHz. Also the hybrid integration in this work is expected to be an attractive solution for high-power amplification using discrete GaN HEMT devices.

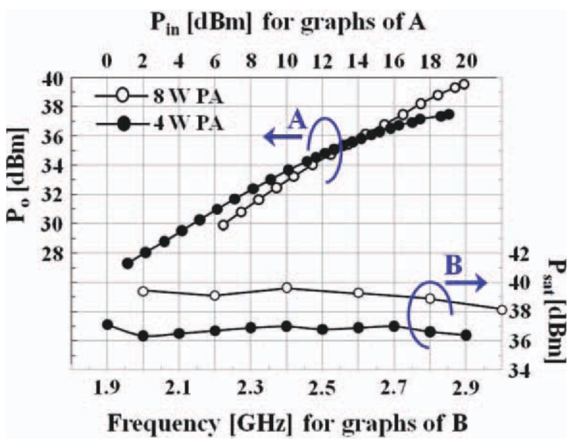

Figure 4 Power measurement results of the fabricated GaN power amplifiers. A: output power, P_o with input power, P_{in} at 2.5 GHz. B: Frequency dependence of the saturated output power, P_s. [Color figure can be viewed in the online issue, which is available at wileyonlinelibrary.com]

ACKNOWLEDGMENTS

This work was supported by the National Research Foundation of Korea Grant funded by the Korean Government (NRF-2010-013-D00049). The author wishes to acknowledge the contribution of the engineers of Wavenics, Inc. who support the semiconductor process and assembly for this work.

REFERENCES

1. U.K. Mishra, L. Shen, T.E. Kazior, and Y.F. Wu, GaN-based RF power devices and amplifiers, Proc IEEE, 96 (2008), 287–305.
2. P. Colantonio, F. Giannini, R. Giofre, and L. Piazzon, High-efficiency ultra-wideband power amplifier in GaN technology, Electron Lett 44 (2008), 130–131.
3. C. Duperrier, M. Campovecchio, L. Roussel, M. Lajugie, and R. Quéré, New design method of uniform and nonuniform distributed power amplifiers, IEEE Trans Microwave Theory Tech 49 (2001), 2494–2500.
4. C. Campbell, C. Lee, V. Williams, M. Kao, H. Tseng, P. Saunier, and T. Balisteri, A wideband power amplifier MMIC utilizing GaN on SiC HEMT technology, IEEE J Solid-State Circuits 44 (2009), 2640–2647.
5. D.W. Kim, I.H. Jeong, H.S. Sung, D.O. Kong, J.S. Lee, C.M. Nam, and Y.S. Kwon, High performance RF passive integration on Si smart substrate, In: IEEE MTT-S Int Microwave Symposium Digest, 2002, pp. 1561–1564.
6. A. Polyakov, S. Sinaga, P.M. Mendes, M. Bartek, J.H. Correia, and J.N. Burghartz, High-resistivity polycrystalline silicon as RF substrate in wafer-level packaging, Electron Lett 41 (2005), 100–101.
7. L. Li, Embedded passives in organic substrate for RF module and assembly characterization, In: Proc. of the Sixth IEEE CPMT Conference on High Density Microsystem Design and Packaging and Component Failure, 2004, pp. 74–82.
8. S.H. Shin and Y.S. Kwon, Selectively anodized aluminum substrates for microwave power module package, In: 55th Electronic Components and Technology, 2005, pp. 1904–1908.
9. K.M. Kim, B. Sohn, J.M. Yook, S.K. Yeo, and Y.S. Kwon, Ultra-thin pocket embedding package for system in package, Electron Lett 43 (2007), 17–18.

A TRIPLE GAIN MODE DIGITALLY CONTROLLED AMPLIFIER IN CMOS PROCESS

Bonghyuk Park and Jaeho Jung
Electronics and Telecommunications Research Institute, 161, Gajeong-dong, Yuseong-gu, Daejeon 305-700, Republic of Korea; Corresponding author: bhpark@etri.re.kr

Received 13 July 2011

ABSTRACT: *A high dynamic range, wide-band triple gain mode amplifier has been developed using CMOS 0.18-μm technology. The proposed low-noise amplifier (LNA) consists of feedback architecture in*